Available online at www.sciencedirect.com
SCIENCE DIRECT®
Journal of Solid State Chemistry 178 (2005) 1968–1972
JOURNAL OF SOLID STATE CHEMISTRY
www.elsevier.com/locate/jssc

Hydrothermal preparation and visible-light photocatalytic activity of Bi_2WO_6 powders

Jiaguo Yu[a,*], Jianfeng Xiong[a], Bei Cheng[a], Ying Yu[b], Jianbo Wang[c]

[a]State Key Laboratory of Advanced Technology for Material Synthesis and Processing, Wuhan University of Technology, Wuhan 430070, PR China
[b]College of Physical Science and Technology, Central China Normal University, Wuhan 430079, PR China
[c]Center for Electron Microscopy, Wuhan University, Wuhan 430072, PR China

Received 17 February 2005; received in revised form 31 March 2005; accepted 2 April 2005
Available online 29 April 2005

Abstract

Bi_2WO_6 powder photocatalyst was prepared using $Bi(NO_3)_3$ and Na_2WO_4 as raw materials by a simple hydrothermal method at 150 °C for 24 h, and then calcined at 300, 400, 500, 600 and 700 °C for 2 h, respectively. The as-prepared samples were characterized with UV-visible diffuse reflectance spectra, fourier transform infrared spectra (FTIR), X-ray diffraction (XRD), scanning electron microscopy (SEM) and N_2 adsorption–desorption measurement. The photocatalytic activity of the samples was evaluated using the photocatalytic oxidation of formaldehyde at room temperature under visible light irradiation. It was found that post-treatment temperature obviously influenced the visible-light photocatalytic activity and physical properties of Bi_2WO_6 powders. At 500 °C, Bi_2WO_6 powder photocatalyst showed the highest visible-light photocatalytic activity due to the samples with good crystallization and high BET surface area.

Keywords: Bi_2WO_6; Preparation; Hydrothermal reaction; Visible-light; Photocatalytic activity; Formaldehyde

1. Introduction

In recent years, a large number of investigations have focused on the semiconductor photocatalyst for its wide applications in solar energy conversion and environmental purification since Fujishima and Honda discovered the photocatalytic splitting of water on the TiO_2 electrodes in 1972 [1–13]. Among various oxide semiconductor photocatalyst, TiO_2 was intensively investigated because of its biological and chemical inertness, strong oxidizing power, nontoxicity and long-term stability against photo and chemical corrosion. However, the fast recombination rate of photogenerated electron/hole pairs hiders the commercialization of this technology [14–18]. Furthermore, TiO_2 is only effective under ultraviolet irradiation ($\lambda < 380$ nm) due to its large band gap (3.2 eV). Usually, sunlight contains about 4% ultraviolet light. Therefore, it is of great interest to develop new visible-light photocatalysts to extend the absorption wavelength range into the visible light region.

In recent years, in the field of water splitting, a new genre of single-phase catalysts has emerged, in which the entire solid rather than just the external surface is involved in catalysis. Layered oxides, such as $K_4Nb_6O_{17}$ [19], $BiInNbO_7$ [20], $Sr_2Nb_2O_7$ [21] and $In_{1-x}Ni_xTaO_4$ [22], etc., had been attracting much attention lately because they are much more active than the generally used TiO_2 or $SrTiO_3$ for photocatalytic water splitting. This kind of photocatalyst belongs to a family of uniform heterogeneous catalyst [23]. However, all the authors used the solid–solid blending method to prepare their samples. James et al. [23] pointed out that the lack of homogeneity of the prepared materials and a drastic decrease in the surface area of the resulting materials by

*Corresponding author. Fax: +86 27 87879468.
E-mail address: jiaguoyu@yahoo.com (J. Yu).

0022-4596/$ - see front matter © 2005 Elsevier Inc. All rights reserved.
doi:10.1016/j.jssc.2005.04.003

high-temperature sintering was the deadly shortcoming of the solid–solid blending method. Recently, visible-light active $Bi_4Ti_3O_{12}$ photocatalyst was synthesized by a chemical solution decomposition (CSD) method [24], which has been proved to be a better method than the solid–solid blending method to prepare a uniform catalyst.

In this study, Bi_2WO_6 powder photocatalyst was prepared using a hydrothermal reaction method. The specific surface area (21.1 m^2/g) of Bi_2WO_6 powders prepared by a hydrothermal process is much higher than that (0.6 m^2/g) of the samples prepared by a solid-state reaction method. To the best of our knowledge, this is the first report on the visible-light photocatalytic active of Bi_2WO_6 powders prepared by a hydrothermal process for the photocatalytic oxidation of formaldehyde at room temperature.

2. Experimental

2.1. Preparation

All chemicals used in this study were received from Shanghai Chemical Regent Factory of China without further purification. $Bi(NO_3)_3 \cdot 5H_2O$ and Na_2WO_4 were firstly dissolved in 150 mL distilled water. After stirring for 15 min, the slurry solution was placed in a 200 mL autoclave with a Teflon liner. The autoclave was maintained at 150 °C for 24 h and then air cooled to room temperature. The yellow precipitate was collected and washed with distilled water. The obtained sample was dried at 100 °C for 5 h and then calcined at 300, 400, 500, 600 and 700 °C for 2 h, respectively.

2.2. Characterization

The X-ray diffraction (XRD) patterns obtained on a diffractometer (type HZG41B-PC) using Cu $K\alpha$ radiation at a scan rate (2θ) of 0.05° s^{-1} were used to determine the identity of any phase present and their crystallite size. The accelerating voltage and the applied current were 15 kV and 20 mA, respectively. The morphologies of Bi_2WO_6 powders were observed by scanning electron microscopy (SEM; type JSM-5610LV) with an accelerating voltage of 20 kV. UV-visible absorption spectra of Bi_2WO_6 powders were obtained for the dry-pressed disk samples using a UV-visible spectrophotometer (Cary 100 Scan Spectrophotometers, Varian, USA). $BaSO_4$ was used as a reflectance standard in the UV-visible diffuse reflectance experiment. Infrared absorption spectra were recorded for KBr disks containing powder sample with an FTIR spectrometer (Nialet-60SXB, American). The Brunauer–Emmett–Teller (BET) surface area (S_{BET}) of the samples was analyzed by nitrogen adsorption in an AUTOSORB-1 (Quantachrome Instruments) nitrogen adsorption apparatus. The dried Bi_2WO_6 powders samples at 100 °C were degassed at 100 °C, and the calcined samples were degassed at 180 °C prior to nitrogen adsorption measurements. The BET surface area was determined by multipoint BET method using the adsorption data in the relative pressure (P/P_0) range of 0.05–0.3 [12,25].

2.3. Measurement of photocatalytic activity

Formaldehyde is a common indoor air pollutant in modern houses, which has been the subject of numerous complaints regarding health disorders, such as nausea, headache, fatigue, dullness and thirst [26,27]. These volatile harmful gases come from plywood, particle-board and adhesives for wall clothes, commonly used in construction and furnishing. In order to improve indoor air quality (IAQ), these volatile organic compounds (VOC) must be eliminated. Therefore, we choose formaldehyde as model contaminate. Photocatalytic oxidations of formaldehyde is based on the following reactions [28]:

$$HCHO + O_2 \rightarrow CO_2 + H_2O. \quad (1)$$

The visible-light photocatalytic activity experiments on the prepared Bi_2WO_6 powders for the oxidations of formaldehyde in air were performed at ambient temperature using a 15 L rectangular photocatalytic reactor. The catalysts were prepared by coating an aqueous suspension of Bi_2WO_6 powders onto three dishes with a diameter of about 9 cm. The weight of catalysts used for each experiment was kept 0.5 g. The dishes containing catalysts were dried in an oven at 100 °C for 2.5 h to evaporate the water and then cooled to room temperature before used. After sample-coated dishes were placed in the reactor, a small amount of formaldehyde was injected into the reactor with a syringe. The reactor was connected to a $CaCl_2$-containing dryer used for controlling the initial humidity in the reactor. The analysis of formaldehyde, carbon dioxide, and water vapor concentration in the reactor was conducted on line with a Photoacoustic IR Multigas Monitor (INNOVA Air Tech Instruments Model 1312). The formaldehyde vapor was allowed to reach adsorption equilibrium with catalysts in the reactor in the dark prior to visible-light irradiation. The initial concentration of formaldehyde after adsorption equilibrium was controlled to 170 ± 10 ppm for all experiments, which remained constant for about 2–3 min until a 15 W daylight lamp (YZ20RR29, Nanjing Lamp Factory) in the reactor was turned on. The distance between the lamp and the Bi_2WO_6-coated dishes was about 5 cm and the total effective irradiation area of the Bi_2WO_6-coated dishes was about 190 cm^2. Integrated intensity in the range 400–500 nm striking the coatings was measured with a UV radiometer (Model: UV-A, made in Photoelectric

Instrument Factory of Beijing Normal University) was $120 \pm 10\,\mu W/cm^2$, while the peak wavelength of UV light was 420 nm. The initial concentration of water vapor was 1.20 ± 0.01vol%, and the initial temperature was $25 \pm 1\,^{\circ}C$. Each set of experiment was carried out for 20 h.

The visible-light photocatalytic activity of the samples can be quantitatively evaluated by comparing the removal efficiency of formaldehyde (R (%)). R (%) was calculated according to the following equation [28]:

$$R(\%) = \frac{[gas]_0 - [gas]_t}{[gas]_0} \times 100\%, \quad (2)$$

where $[gas]_0$ and $[gas]_t$ represent the initial equilibrium concentration and reaction concentration of formaldehyde, respectively.

3. Results and discussion

XRD is used to investigate the phase structures and average crystallite size of the as-prepared Bi_2WO_6 powders. Fig. 1 shows the XRD patterns of Bi_2WO_6 powders calcined at different temperatures. It can be seen that the as-prepared sample at low temperature (below 300 °C) shows weak crystallization. With increasing calcination temperature, the diffraction peak intensity of Bi_2WO_6 obviously increases and the width of the peak becomes gradually narrower, which is due to the growth of crystallites and enhancement of crystallization. At 400 °C, the diffraction peaks of the samples can be indexed with the russellite phase of Bi_2WO_6 (JCPDS Card: 26-1044). It is well known that the crystallization and the surface area of the photocatalyst are two important factors influencing the photocatalytic activity. However, with the improvement of crystallization, the crystallites become larger, the BET surface areas (as shown in Table 1) of the samples decrease. Figs. 2(a) and (b) show the SEM photographs of Bi_2WO_6 powders calcined at 500 and 700 °C, respectively. It could be seen that the Bi_2WO_6 powders calcined at 500 °C had smaller particle size. On the contrary, the Bi_2WO_6 powders calcined at 700 °C displayed greater particle size due to sintering between smaller particles. This also indicated that the specific surface areas of the Bi_2WO_6 powders decrease with increasing calcination temperature. Therefore, we try to find an optimal temperature at which the photocatalyst shows the highest photocatalytic activity.

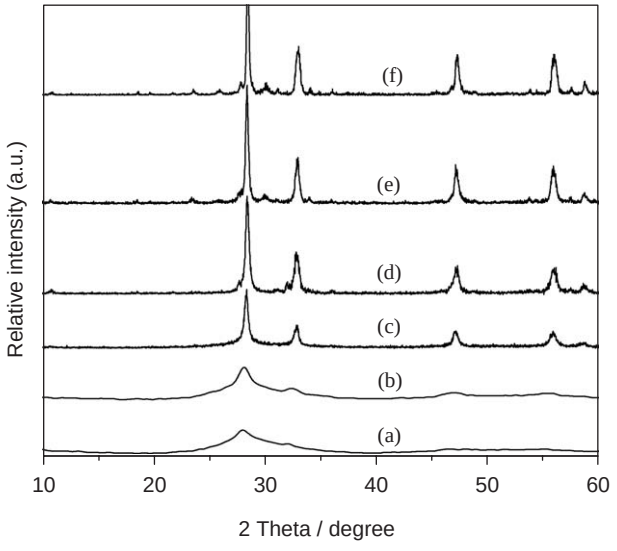

Fig. 1. XRD patterns of Bi_2WO_6 powders calcined at (a) 100, (b) 300, (c) 400, (d) 500, (e) 600, (f) 700 °C for 2 h.

Figs. 3(a–d), show the UV-visible diffuse reflectance spectra of Bi_2WO_6 powders calcined at 400, 500, 600 and 700 °C, respectively. A significant increase in the absorption wavelengths lower than about 460 nm can be assigned to the intrinsic band gap absorption of Bi_2WO_6. With increasing calcination temperature, the samples show a stronger absorption in the UV-visible range and a red shift in the band gap transition. The red shift is ascribed to the increase in crystallite size.

The band gap energy can be estimated from a plot of $(\alpha)^{1/2}$ versus photon energy ($h\nu$). The intercept of the tangent to the plot will give a good approximation of the band gap energy for indirect band gap materials such as TiO_2 [11,29–31]. The absorption coefficient α can be calculated from the measured absorbance (A) using the following equation:

$$\alpha = \frac{2.303\rho 10^3}{lcM} A, \quad (3)$$

where the density $\rho = 9.512\,g\,cm^{-3}$, molecular weight $M = 697.81\,g\,mol^{-1}$, c is the molar concentration of Bi_2WO_6, and l is the optical path length [11,30]. Plots of the $(\alpha)^{1/2}$ versus photon energy ($h\nu$) are shown in Fig. 4. The band gap energies estimated from the intercept of the tangents to the plots are 2.77, 2.64, 2.52 and 2.50 eV for Bi_2WO_6 calcined at 400, 500, 600 and 700 °C, respectively. The band gap energies decrease with increasing calcination temperature. This indicates that Bi_2WO_6 has a suitable band gap for photocatalytic decomposition of organic contaminants under visible light irradiation.

FT-IR spectra of Bi_2WO_6 powder samples calcined at various temperatures are shown in Fig. 5. The Bi_2WO_6 samples show main absorption bands at 400–1000 cm^{-1}, which are attributed to Bi–O, W–O stretching and W–O–W bridging stretching modes [32,33]. The peaks at 1384 and 1640 cm^{-1} are attributed to bending vibrations of N–O and O–H, respectively. The IR spectrum of the sample dried at 100 °C reveals that W–O, Bi–O, N–O groups exist in the as-prepared sample. Since hydrothermal reaction is carried out in an aqueous solution system, the prepared samples easily adsorb water

Table 1
BET surface area and average crystallite size of Bi_2WO_6 powders calcined at various temperatures

Calcination temperature (°C)	100	400	500	600	700
Surface area (m^2/g)	21.14	13.79	10.21	5.458	2.197
Crystallite size (nm)	9.1	27.9	28.5	52.0	72.9

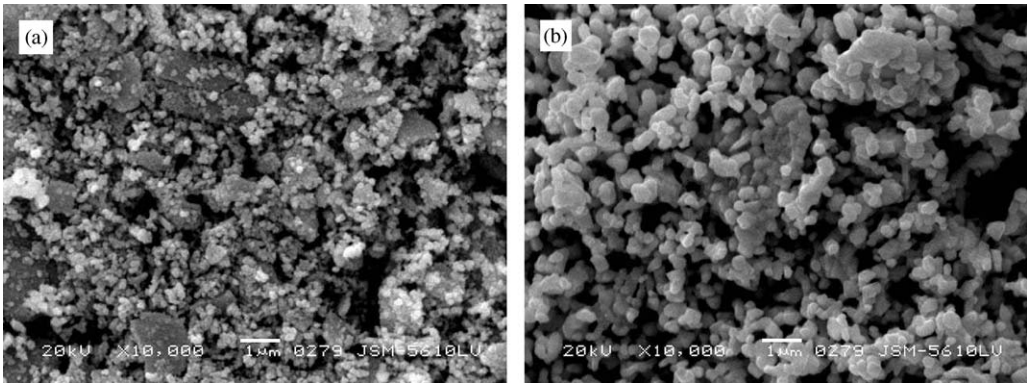

Fig. 2. SEM photographs of Bi_2WO_6 powders calcined at (a) 500 and (b) 700 °C for 2 h.

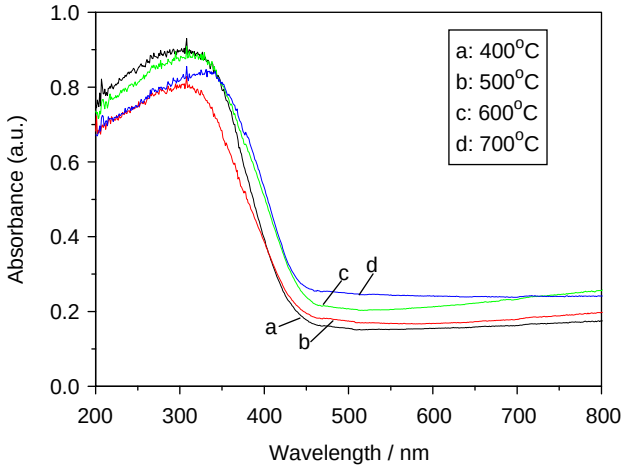

Fig. 3. UV-Vis diffuse reflectance spectra of Bi_2WO_6 powders calcined at (a) 400, (b) 500, (c) 600 and (d) 700 °C for 2 h.

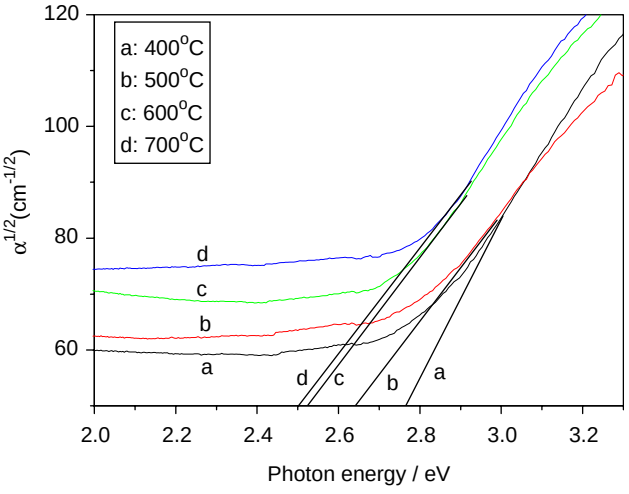

Fig. 4. Plots of the $(\alpha)^{1/2}$ versus photon energy ($h\nu$) for Bi_2WO_6 powders calcined at (a) 400, (b) 500, (c) 600 and (d) 700 °C for 2 h.

molecules. NO_3^- ions come from the raw material. The intensities of O–H and N–O vibration bands decrease and the intensities of W–O and Bi–O vibration bands increase with increasing calcinations temperature. NO_3^- ions almost completely disappeared at 500 °C. There is a small peak existing at about 1640 cm^{-1} in all curves, which corresponds to the hydroxyl groups in Bi_2WO_6 powders. This shows that the hydroxyl groups always exist in Bi_2WO_6 powders.

Fig. 6 shows the dependence of visible-light photocatalytic activity on calcination temperature. It can be seen that the as-prepared sample at 100 °C shows weak visible-light photocatalytic activity with formaldehyde removal efficiency of 8.32%. This may be due to the fact that at 100 °C, although the sample had high surface area, Bi_2WO_6 shows weak crystallization. With increasing calcination temperature, the photocatalytic activity of Bi_2WO_6 increases due to the enhancement of Bi_2WO_6 crystallization. At 500 °C, the photocatalyst reaches the highest photocatalytic activity with formaldehyde removal efficiency of 68.8% in 20 h. This is due to the samples with good crystallization and high surface area. However, with further increasing calcination temperature, the photocatalystic activity decreases due to the decrease of BET surface area of Bi_2WO_6 samples.

4. Conclusions

Visible-light active Bi_2WO_6 powder photocatalyst could be prepared by a simple hydrothermal reaction

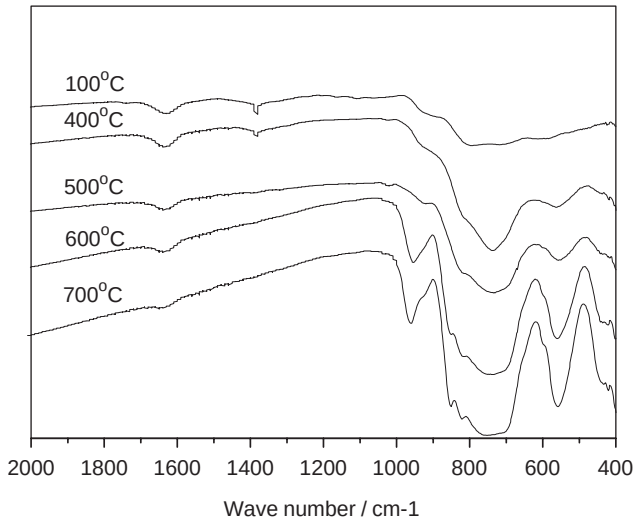

Fig. 5. FT-IR spectra of the Bi_2WO_6 powder samples calcined at various temperatures.

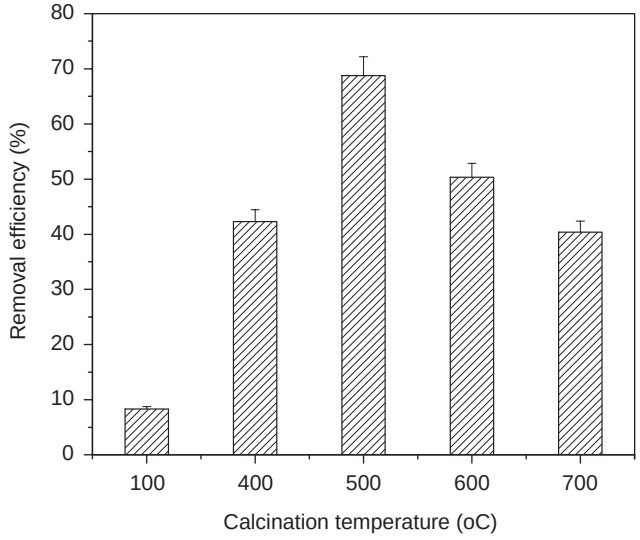

Fig. 6. The photocatalytic activity of Bi_2WO_6 powders calcined at various temperatures under visible light irradiation.

at 150 °C. Post-treatment temperatures obviously influenced the visible-light photocatalytic activity and physical properties of Bi_2WO_6 powders. At 500 °C, Bi_2WO_6 powder photocatalyst showed the highest visible-light photocatalytic activity due to the samples with good crystallization and high BET surface area. This work may provide new insights into the development of novel visible-light photocatalyst.

Acknowledgment

This work was partially supported by the National Science Foundation of China (50272049 and 20473059), this work was also financially supported by the Excellent Young Teachers Program of MOE of China, Project-Sponsored by SRF for ROCS of SEM of China, Key Project of State Key Laboratory of Advanced Technology for Materials Synthesis and Processing (WUT2004Z03).

References

[1] K. Honda, A. Fujishima, Nature 238 (1972) 37.
[2] H. Tada, M. Yamamoto, S. Ito, Langmuir 15 (1999) 3699.
[3] M.A. Fox, M.T. Dulay, Chem. Rev. 93 (1993) 341.
[4] M.R. Hoffmann, S.T. Martin, W. Choi, D.W. Bahnemann, Chem. Rev. 95 (1995) 69.
[5] A. Fujishima, T.N. Rao, D.A. Tryk, J. Photochem. Photobiol. C: Photochem. Rev. 1 (2000) 1.
[6] J.G. Yu, H.G. Yu, B. Cheng, X.J. Zhao, J.C. Yu, W.K. Ho, J. Phys. Chem. B 107 (2003) 13871.
[7] J.C. Zhao, T.X. Wu, K.Q. Wu, K. Oikawa, H. Hidaka, N. Serpone, Environ. Sci. Technol. 32 (1998) 2394.
[8] Y.M. Xu, C.H. Langford, Langmuir 17 (2001) 897.
[9] J.C. Yu, J.G. Yu, W.K. Ho, L.Z. Zhang, Chem. Commun. (2001) 1942.
[10] F.B. Li, X.Z. Li, C.H. Ao, M.F. Hou, S.C. Lee, Appl. Catal. B 54 (2004) 275.
[11] J.C. Yu, J.G. Yu, W.K. Ho, Z.T. Jiang, L.Z. Zhang, Chem. Mater. 14 (2002) 3808.
[12] J.G. Yu, J.C. Yu, M.K.P. Leung, W.K. Ho, B. Cheng, X.J. Zhao, J.C. Zhao, J. Catal. 217 (2003) 69.
[13] F.B. Li, X.Z. Li, M.F. Hou, Appl. Catal. B 48 (2004) 185.
[14] A. Linsebigler, L. Lu, G. Yates, J.T. Jr, Chem. Rev. 95 (1995) 735.
[15] J.G. Yu, J.C. Yu, B. Cheng, S.K. Hark, K. Iu, J. Solid State Chem. 174 (2003) 372.
[16] J.G. Yu, J.C. Yu, B. Cheng, X.J. Zhao, Sci. China Ser. B 46 (2003) 549.
[17] J.G. Yu, J.C. Yu, Chin. J. Chem. 21 (2003) 994.
[18] C. Wang, J. Zhao, X. Wang, B. Mai, G. Sheng, P. Peng, J. Fu, Appl. Catal. B: Environ. 39 (2002) 269.
[19] S. Uchida, Y. Yamamoto, Y. Fujishiro, A. Watanabe, O. Ito, T. Sato, J. Chem. Soc. Dalton Trans. 93 (1997) 3229.
[20] Z. Zou, J.H. Ye, H. Arakawa, Chem. Mater. 13 (2001) 1765.
[21] G.K. Hyum, W.H. Dong, K. Jindo, G.K. Yong, S.L. Jae, Chem. Commun. (1999) 1077.
[22] Z. Zou, J.H. Ye, K. Sayama, H. Arakawa, Nature 414 (2001) 625.
[23] A.S. James, C. Cristian, C. Adriana, Chem. Rev. 95 (1995) 477.
[24] W.F. Yao, H. Wang, X.H. Xu, S.X. Shang, Y. Hou, Y. Zhang, M. Wang, Mater. Lett. 57 (2003) 1899.
[25] K.S.W. Sing, D.H. Everett, R.A.W. Haul, L. Moscou, R.A. Pierotti, J. Rouquerol, T. Siemieniewska, Pure Appl. Chem. 57 (1985) 603.
[26] M.E. Zorn, D.T. Tompkins, W.A. Zeltner, M.A. Anderson, Appl. Catal. B 23 (1999) 1.
[27] Y. Sekine, Atmos. Environ. 36 (2002) 5543.
[28] J.G. Yu, M.H. Zhou, B. Cheng, H.G. Yu, X.J. Zhao, J. Mol. Catal. A 227 (2005) 75.
[29] M.M. Rahman, K.M. Krishna, T. Soga, T. Jimbo, M. Umeno, J. Phys. Chem. Solids 60 (1999) 201.
[30] C. Kormann, D.W. Bahnemann, M.R. Hoffman, J. Phys. Chem. 92 (1988) 5196.
[31] J.G. Yu, J.C. Yu, W.K. Ho, Z.T. Jiang, New J. Chem. 26 (2002) 607.
[32] M.L. Calzada, R. Sirera, F. Carmona, J. Am. Soc. 78 (7) (1995) 1802.
[33] M.F. Daniel, B. Desbat, J.C. Lassegus, J. Solid Chem. 73 (1988) 127.